

# Dielectric properties and abnormal C-V characteristics of $\text{Ba}_{0.5}\text{Sr}_{0.5}\text{TiO}_3\text{-Bi}_{1.5}\text{ZnNb}_{1.5}\text{O}_7$ composite thin films grown on MgO (001) substrates by pulsed laser deposition

Huyong Tian,<sup>a)</sup> Yu Wang, Danyang Wang, Jun Miao, Jianquan Qi, H. L. W. Chan, and C. L. Choy

*Materials Research Center, Department of Applied Physics, The Hong Kong Polytechnic University, Hung Hom, Kowloon, Hong Kong, China*

(Received 17 February 2006; accepted 17 August 2006; published online 3 October 2006)

Highly *c*-axis oriented  $\text{Ba}_{0.5}\text{Sr}_{0.5}\text{TiO}_3$ -based composite thin films were grown on MgO (001) single-crystal substrates by pulsed laser deposition and the in-plane dielectric properties of the films evaluated. X-ray diffraction characterization revealed a good crystallinity. The dielectric constant and loss were found to be 200 and 0.001–0.007 at room temperature, respectively. The butterfly-shaped *C*-*V* characteristic curve evidenced an enhanced in-plane dielectric tunability of >90% in the films at 1 MHz under a dc bias field of 0.8 MV/cm. A brief discussion is given on the abnormal *C*-*V* curves. Various tunable microwave applications of  $\text{Ba}_{0.5}\text{Sr}_{0.5}\text{TiO}_3\text{-Bi}_{1.5}\text{ZnNb}_{1.5}\text{O}_7$  composite thin films are expected. © 2006 American Institute of Physics.  
[DOI: 10.1063/1.2358934]

In recent years, there is a rapidly growing demand for electrically tunable microwave devices in advanced radar and communication devices. The high dielectric nonlinearity (i.e., the strong dependence of permittivity on electric field) of ferroelectric materials with perovskite structure has made them promising candidates for these applications. Many research efforts have been focused on the ferroelectric  $\text{Ba}_x\text{Sr}_{1-x}\text{TiO}_3$  (BST) systems.<sup>1,2</sup> Since many important new generation elements will depend on the use of thin films to achieve improved and enhanced performance, a considerable amount of research work has been done to develop tunable ferroelectric thin films for fabricating electric field dependent microwave devices. Generally, ferroelectrics with Curie temperature below the operating temperature are employed in practical device applications because the paraelectric state of ferroelectric materials has lower dielectric loss due to the disappearance of hysteresis. Another effective way, which has been done to reduce the dielectric loss of ferroelectric materials, is to dope selected low loss oxides (e.g.,  $\text{MgO}$ ,<sup>3</sup>  $\text{Al}_2\text{O}_3$ ,<sup>4</sup> etc.) into ferroelectric materials.

A nonferroelectric thin film material,  $\text{Bi}_{1.5}\text{ZnNb}_{1.5}\text{O}_7$  (BZN), which has the cubic pyrochlore structure and a moderate permittivity ( $\sim 150$ ), has attracted considerable interest due to its very low loss ( $\sim 5 \times 10^{-4}$ ) and large tunability (55% at 2.4 MV/cm) at room temperature.<sup>5–7</sup> These properties offer us a good opportunity to use BZN as a dopant to substitute the above mentioned oxides, which are all nontunable and of relatively low dielectric constant to improve the microwave dielectric properties of BST thin films.<sup>8</sup> It is logical to explore BZN doped composite thin films as modifiers for their electrical properties. In this letter, we report the preparation and characterization of BST-BZN composite thin films using pulsed laser deposition (PLD) technique. Moderate dielectric constant, high dielectric tunability, and low dielectric loss were obtained, showing that these com-

posites are promising materials for use in tunable microwave applications.

To obtain BST (usually sintered at  $>1300^\circ\text{C}$ ) and BZN [usually sintered below  $1000^\circ\text{C}$  (Refs. 9–11)] PLD targets using the traditional solid-state reaction processes, nano-scaled BST powder with an average particle size of about 17–25 nm (Refs. 12 and 13) was used in order that the combined BST-BZN target can be sintered at a relatively low temperature. In this study, stoichiometric compositions of BZN derived from reagent grade oxides of  $\text{Bi}_2\text{O}_3$ ,  $\text{ZnO}$ , and  $\text{Nb}_2\text{O}_5$  were mixed and ball ground in water for 12 h, dried, and then calcined at  $800^\circ\text{C}$  for 4 h. Approximately 20 wt % BZN was used to prepare the composite target, the mixtures including 80 wt % of nano-BST powders were ball ground for 4 h, dried, and then pressed with a pressure of 2–3 ton/cm<sup>2</sup>. The PLD target (BST-BZN20) was sintered at  $1050^\circ\text{C}$  for 2 h in atmosphere.

The composite thin films were grown on MgO (001) single-crystal substrates using a KrF excimer laser (Lambda Physik COMPex 205) with a wavelength of 248 nm. The laser was set to a 10 Hz repetition rate and 3 J/cm<sup>2</sup> energy density was used to irradiate a rotating target. The target-substrate distance was 50 mm. Deposition was performed in a vacuum chamber that was first evacuated to a base pressure of  $2 \times 10^{-5}$  Torr and then back filled with pure oxygen and/or argon, keeping the working pressure near 100 mTorr.

The substrate temperature ( $\sim 650^\circ\text{C}$ ) was determined by a thermocouple embedded directly underneath the substrate in the face plate of the substrate holder. After deposition, the samples ( $\sim 150$  nm) were kept in a chamber at the deposition temperature for 10 min with 200 mTorr of oxygen ambience by inputting pure oxygen. The films were then cooled down to room temperature at the same oxygen ambience. Phase analyses of target and thin films were performed by x-ray diffraction (XRD) using a Philips x-ray diffractometer (model: X'Pert-Pro MPD) with Cu  $K\alpha$  radiation. The out-of-plane alignment of the composite thin film was measured by its diffraction from the (001) plane and by rotating this sample about the (001) axis (labeled  $\omega$ ). The

<sup>a)</sup>Electronic mail: aphytian@polyu.edu.hk

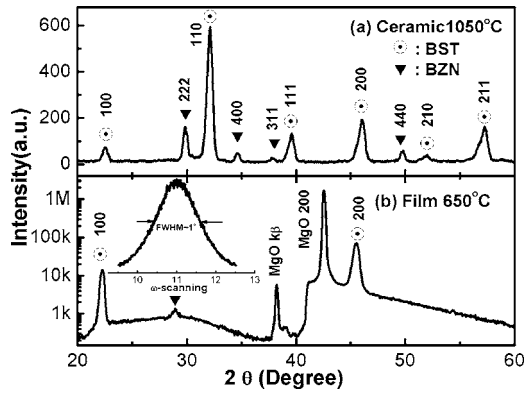


FIG. 1. XRD patterns of  $\theta/2\theta$  scan from (a) BST-BZN20 composite ceramic sintered at 1050 °C for 2 h and (b) thin film deposited on MgO (001) substrate. The inset in (b) is the rocking curve of BST along (001) peak.

relative permittivity and loss were measured from 1 kHz to 1 MHz and the samples were fixed in a cryostat (Oxford Instrument) with the temperature controlled to vary from  $-195$  to  $120$  °C. The  $C$ - $V$  characteristics were measured under a bias field of  $0.8$ – $1.3$  MV/cm at room temperature.

According to differential scanning calorimetry analysis of pure BZN ceramic powder (not shown here), it shows exothermic peaks between  $760$  and  $825$  °C, meaning the solid-state reaction happens in this temperature range. It was speculated that the final compound BZN was formed from  $850$  °C to higher temperatures.<sup>10,11</sup> However, the product in the compound is not a pure single phase, i.e., the coexistence of cubic pyrochlore  $\text{Bi}_{1.5}\text{ZnNb}_{1.5}\text{O}_7$  and monoclinic  $\text{Bi}_2\text{Zn}_{2/3}\text{Nb}_{4/3}\text{O}_7$  in the powders calcined at  $800$  °C. The monoclinic phases disappeared when the samples were sintered over  $1000$  °C. Higher sintering temperature leads to the formation of some protuberances on the surface and some voids in the bulk. BST-BZN20 composite ceramics were sintered at  $1050$  °C for 2 h, and the XRD pattern in Fig. 1(a) shows the presence of a cubic pyrochlore structure for the BZN phase in the sample. Figure 1(b) is an XRD pattern of the BST-BZN20 thin films on a MgO substrate. It shows that, in addition to a peak around  $30^\circ$  from BZN, only the {001} peaks of BST appear in the  $\theta/2\theta$  scan pattern, which shows that BST has a pure perovskite phase. The rocking curve measurement of the BST (001) reflection, as shown in the inset of Fig. 1(b), indicating a  $c$ -axis textured growth revealed that the full width at half maximum is about  $1^\circ$ .

The in-plane dielectric characterization was carried out using coplanar interdigital electrodes (IDEs), as shown in Fig. 2. The top electrodes constituting an interdigitated finger pattern were prepared by rf sputtering of Au with a thickness of  $200$  nm on the composite thin film surface followed by patterning using standard photolithography and wet chemical etching process. The IDE structure and dimensions could be found elsewhere.<sup>14</sup> The metal-dielectric-metal structure can be modeled by a series of alternating thin parallel electrodes. Considering the given dimensions and materials constants, the capacitance per unit area of such a structure can be estimated using the following formulas:<sup>15</sup>

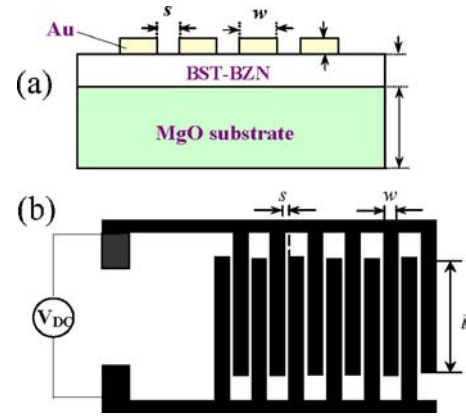


FIG. 2. (Color online) (a) Cross-sectional view and (b) top view of the interdigitated finger pattern.

$$C = \frac{\epsilon_0(\epsilon_d + \epsilon_s)}{(w + s)} \frac{\pi}{(\ln 2 + 2 \arctan x)}, \quad (1)$$

where  $x = \cos^{1/4}(2u)/\cos u$  and  $u = \pi/4(s/w + 1)$ .  $\epsilon_0$  is the permittivity of free space, and  $\epsilon_d$  and  $\epsilon_s$  are the dielectric constants for the dielectric layer and the substrate, respectively. The finger and gap widths are denoted by  $w$  and  $s$ , respectively.

A frequency dispersion of dielectric properties was observed where the permittivity value dropped and the maxima in the dielectric constant curves of pure BZN were found to decrease and shift to higher temperature with increasing measuring frequency.<sup>5–7</sup> The permittivity (a) and loss (b) of BST-BZN20 thin film were evaluated between  $1$  kHz and  $1$  MHz, as shown in Fig. 3. The dielectric constants increased at different frequencies, instead of dropping, when increasing the temperature beyond the maximum points. However, the corresponding maxima of loss shifted to higher temperature with increasing measuring frequency. It was speculated that there exist different mechanisms in this process. At lower temperature, the relaxation tendency was identical to pure BZN.<sup>5,6</sup> In BZN, the relaxation might stem from the hopping of dynamically disordered Bi and Zn atoms at the A sites and hopping of O' atoms among 12 sites.<sup>16</sup> It is visible as an increase in loss peaks from  $-177.6$  °C ( $1$  kHz) to  $-14.5$  °C ( $1$  MHz) with increasing

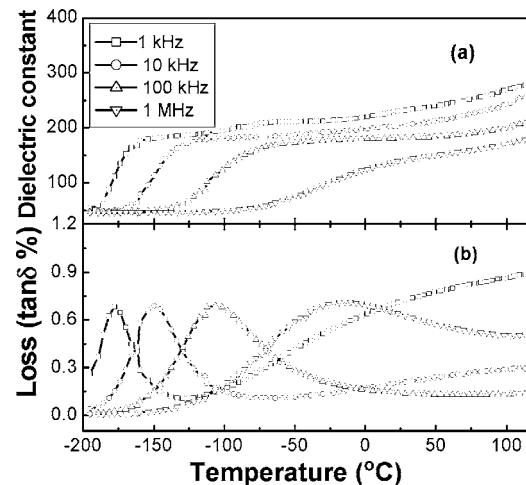


FIG. 3. (a) Permittivity and (b) loss of BST-BZN20 composite thin film as a function of temperature and frequency between  $1$  kHz and  $1$  MHz.

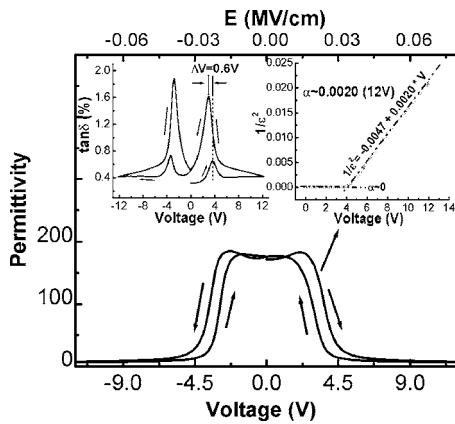


FIG. 4. Bias field dependence of permittivity of BST-BZN20 composite thin film in IDE structure measured at 1 MHz and room temperature. The left inset shows the corresponding loss and the right inset shows the relationship of  $1/C^2(1/\epsilon^2) \sim V$ .

frequency. However, the relatively broader low-temperature dielectric relaxation was demonstrated in BST-BZN20 composite thin film. A uniform distribution of random fields has been suggested to be responsible for the dielectric relaxation.<sup>17</sup> An increase in the dielectric constants was likely attributed to variations of activation energy, which causes more movements, e.g., thermal hopping increases at elevated temperatures. From a device impedance matching point of view, moderate dielectric constant and low loss tangent are required. The dielectric constants are between 150 and 250 in the frequency range of 1 kHz to 1 MHz at room temperature and losses are from 0.001 to 0.007, which are proper for microwave device applications.

Figure 4 shows the capacitance–dc-bias voltage ( $C$ - $V$ ) curves obtained with a dc bias field of 0.8 MV/cm (12 V) at the frequency of 1 MHz with small ac signal amplitude of 50 mV. In the initial scanning from 0 to 12 V, a small peak appeared and then a large peak appeared after decreasing from the maxima to 0 V. The difference between the two peaks is 0.6 V. The similar hysteresis character was also observed when scanning continually from 0 to –12 V and then from –12 to 0 V, as shown in the left inset. The presence of doubly positive oxygen vacancies are the most probable source of positive charges, which could cause the observed shift.<sup>17</sup> The  $C(\epsilon)$ - $V$  curve looks quite different from regular ones observed in single phase ferroelectric thin films. Under a relatively small dc bias (i.e., sweeping up from –2.25 to 2.4 V and sweeping down from 2.25 to –2.4 V), the dielectric constant remained almost unchanged ( $\epsilon \sim 180$ ). It was speculated that the built-in potential played an important role at a low bias field and neutralized the effect of the bias field up to saturation.<sup>18</sup> As increasing the bias field, the dramatic decrease in capacitance indicated the existence of symmetrical Schottky barriers. The dependence of the capacitance on the voltage shows a strongly nonlinear character. The interface capacitance formed by the Schottky barrier results in clear hysteresis effect and its symmetry. It can be assumed that the MFM configuration behaves as a normal Schottky contact. The relationship of  $1/C^2 \sim V$  or  $1/\epsilon^2 \sim V$  can be employed to evaluate the like semiconductor Schottky contact.<sup>19</sup> As expected, the linear variation was shown with the slope of 0.0020 for the film at a bias field of 0.8 MV/cm,

as shown in the inset of Fig. 4. An onset temperature exists (i.e., 4 V); the slope is close to zero below it. The characterization of dielectric constant depending on the bias dc voltage provides a main evaluation in tunable devices. The tunability of dielectric constant of the thin films is defined as  $[\epsilon(0) - \epsilon(E)]/\epsilon(0)$ , where  $\epsilon(E)$  is the dielectric constant at the maximum applied field and  $\epsilon(0)$  is the dielectric constant at zero bias. Under a dc bias of 0.8 MV/cm, the in-plane dielectric tunability is >90%. The mechanism responsible for the irregular  $C$ - $V$  curve and high tunability of the composite thin film, however, is not yet clear due to the very complicated composition and microstructure. More microstructure analyses will be conducted to reveal the mechanism for the abnormal dielectric behavior.

In summary, we have shown that the BST-BZN20 composite thin film was textured and highly  $c$  axis oriented by PLD at 650 °C. The dielectric properties were investigated along the in-plane direction using IDE pattern. The obvious dielectric relaxation was observed at low temperature, and the maxima in the dielectric loss tangent curves of the composite thin film were found to decrease and shift to higher temperature with increasing measuring frequency. The dielectric constant and loss are 200 and 0.001–0.007 at room temperature, respectively. Abnormal butterfly-shaped  $C$ - $V$  curves with four peaks were obtained. The high dielectric tunability of over 90% at a bias field 0.8 MV/cm may make these films promising candidates for tunable capacitor applications.

This research was supported by the programs (K-ZP51, 1-BBZ3, and 1-A302) of The Hong Kong Polytechnic University.

- <sup>1</sup>S. Zafar, R. E. Jones, P. Chu, B. White, B. Jiang, D. Taylor, P. Zurcher, and S. Gillespie, *Appl. Phys. Lett.* **72**, 2820 (1998).
- <sup>2</sup>Z. Yuan, Y. Lin, J. Weaver, X. Chen, C. L. Chen, G. Subramanyam, J. C. Jiang, and E. L. Meletis, *Appl. Phys. Lett.* **87**, 152901 (2005).
- <sup>3</sup>M. W. Cole, W. D. Nothwang, C. Hubbard, E. Ngo, and M. Ervin, *J. Appl. Phys.* **93**, 9218 (2003).
- <sup>4</sup>K. B. Chong, L. B. Kong, L. F. Chen, L. Yan, C. Y. Tan, T. Yang, C. K. Ong, and T. Osipowicz, *J. Appl. Phys.* **95**, 1416 (2004).
- <sup>5</sup>J. W. Lu, D. O. Klenov, and S. Stemmer, *Appl. Phys. Lett.* **84**, 957 (2004).
- <sup>6</sup>A. K. Tagantsev, J. W. Lu, and S. Stemmer, *Appl. Phys. Lett.* **86**, 032901 (2005).
- <sup>7</sup>D. Liu, Y. Liu, S. Q. Huang, and X. Yao, *J. Am. Ceram. Soc.* **76**, 2129 (1993).
- <sup>8</sup>L. Yan, L. B. Kong, L. F. Chen, K. B. Chong, C. Y. Tan, and C. K. Ong, *Appl. Phys. Lett.* **85**, 3522 (2004).
- <sup>9</sup>H. Wang, X. Wang, and X. Yao, *J. Am. Ceram. Soc.* **80**, 2745 (1997).
- <sup>10</sup>H. Wang, X. L. Wang, and X. Yao, *Ferroelectrics* **195**, 19 (1997).
- <sup>11</sup>H. Wang, X. Yao, L. Y. Zhang, and F. Xia, *Ferroelectrics* **229**, 95 (1999).
- <sup>12</sup>J. Q. Qi, L. T. Li, Y. L. Wang, and Z. L. Gui, *J. Cryst. Growth* **260**, 551 (2004).
- <sup>13</sup>H. Y. Tian, J. Q. Qi, Y. Wang, J. Wang, H. L. W. Chan, and C. L. Choy, *Nanotechnology* **16**, 47 (2005).
- <sup>14</sup>D. Y. Wang, Y. Wang, X. Y. Zhou, H. L. W. Chan, and C. L. Choy, *Appl. Phys. Lett.* **86**, 212904 (2005).
- <sup>15</sup>D. L. Rogers, *J. Lightwave Technol.* **9**, 1635 (1991).
- <sup>16</sup>S. Kamba, V. Porokhonkyy, A. Pashkin, V. Bovtun, and J. Petzelt, *Phys. Rev. B* **66**, 054106 (2002).
- <sup>17</sup>S. C. Roy, G. L. Sharma, M. C. Bhatnagar, R. Manchanda, V. R. Balakrishnan, and S. B. Samanta, *Appl. Surf. Sci.* **236**, 306 (2004).
- <sup>18</sup>L. Pintilie, M. Liscu, and M. Alexe, *Appl. Phys. Lett.* **86**, 192902 (2005).
- <sup>19</sup>D. K. Schroeder, *Semiconductor Material and Device Characterization* (Wiley-Interscience, New York, 1998), Chap. 3, pp. 170–173.

Applied Physics Letters is copyrighted by the American Institute of Physics (AIP). Redistribution of journal material is subject to the AIP online journal license and/or AIP copyright. For more information, see <http://ojps.aip.org/aplo/aplcr.jsp>